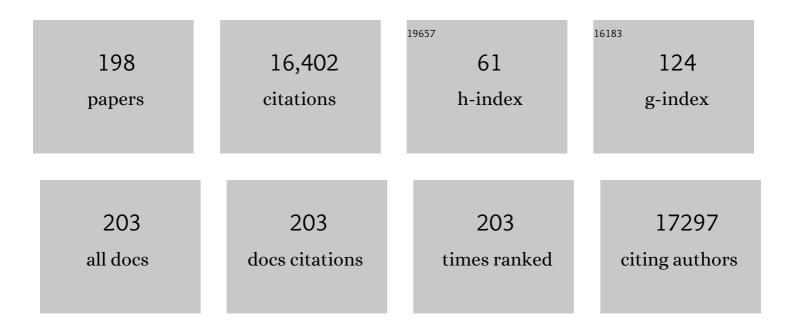
## Tonio Buonassisi

List of Publications by Year in descending order

Source: https://exaly.com/author-pdf/9575955/publications.pdf Version: 2024-02-01



#	Article	IF	CITATIONS
1	Promises and challenges of perovskite solar cells. Science, 2017, 358, 739-744.	12.6	1,510
2	23.6%-efficient monolithic perovskite/silicon tandem solar cells with improved stability. Nature Energy, 2017, 2, .	39.5	1,204
3	Identifying defect-tolerant semiconductors with high minority-carrier lifetimes: beyond hybrid lead halide perovskites. MRS Communications, 2015, 5, 265-275.	1.8	662
4	Semi-transparent perovskite solar cells for tandems with silicon and CIGS. Energy and Environmental Science, 2015, 8, 956-963.	30.8	630
5	An interface stabilized perovskite solar cell with high stabilized efficiency and low voltage loss. Energy and Environmental Science, 2019, 12, 2192-2199.	30.8	542
6	A 2-terminal perovskite/silicon multijunction solar cell enabled by a silicon tunnel junction. Applied Physics Letters, 2015, 106, .	3.3	488
7	Pathways for solar photovoltaics. Energy and Environmental Science, 2015, 8, 1200-1219.	30.8	385
8	Hybrid Organic–Inorganic Perovskites (HOIPs): Opportunities and Challenges. Advanced Materials, 2015, 27, 5102-5112.	21.0	372
9	Technology and Market Perspective for Indoor Photovoltaic Cells. Joule, 2019, 3, 1415-1426.	24.0	316
10	Methylammonium Bismuth Iodide as a Leadâ€Free, Stable Hybrid Organic–Inorganic Solar Absorber. Chemistry - A European Journal, 2016, 22, 2605-2610.	3.3	312
11	Terawatt-scale photovoltaics: Trajectories and challenges. Science, 2017, 356, 141-143.	12.6	303
12	Searching for "Defect-Tolerant―Photovoltaic Materials: Combined Theoretical and Experimental Screening. Chemistry of Materials, 2017, 29, 4667-4674.	6.7	275
13	Ten-percent solar-to-fuel conversion with nonprecious materials. Proceedings of the National Academy of Sciences of the United States of America, 2014, 111, 14057-14061.	7.1	262
14	Homogenized halides and alkali cation segregation in alloyed organic-inorganic perovskites. Science, 2019, 363, 627-631.	12.6	258
15	Atomic Layer Deposited Gallium Oxide Buffer Layer Enables 1.2 V Open ircuit Voltage in Cuprous Oxide Solar Cells. Advanced Materials, 2014, 26, 4704-4710.	21.0	242
16	3.88% Efficient Tin Sulfide Solar Cells using Congruent Thermal Evaporation. Advanced Materials, 2014, 26, 7488-7492.	21.0	227
17	SnS thin-films by RF sputtering at room temperature. Thin Solid Films, 2011, 519, 7421-7424.	1.8	224
18	Open-Circuit Voltage Deficit, Radiative Sub-Bandgap States, and Prospects in Quantum Dot Solar Cells. Nano Letters, 2015, 15, 3286-3294.	9.1	223

2

#	Article	IF	CITATIONS
19	Accelerating Materials Development via Automation, Machine Learning, and High-Performance Computing. Joule, 2018, 2, 1410-1420.	24.0	210
20	Room-temperature sub-band gap optoelectronic response of hyperdoped silicon. Nature Communications, 2014, 5, 3011.	12.8	202
21	Light-induced water oxidation at silicon electrodes functionalized with a cobalt oxygen-evolving catalyst. Proceedings of the National Academy of Sciences of the United States of America, 2011, 108, 10056-10061.	7.1	195
22	Accelerated Development of Perovskite-Inspired Materials via High-Throughput Synthesis and Machine-Learning Diagnosis. Joule, 2019, 3, 1437-1451.	24.0	187
23	Engineering metal-impurity nanodefects for low-cost solar cells. Nature Materials, 2005, 4, 676-679.	27.5	185
24	Fast and interpretable classification of small X-ray diffraction datasets using data augmentation and deep neural networks. Npj Computational Materials, 2019, 5, .	8.7	177
25	Investigation of Bismuth Triiodide (Bil <sub>3</sub> ) for Photovoltaic Applications. Journal of Physical Chemistry Letters, 2015, 6, 4297-4302.	4.6	176
26	Ultrathin amorphous zinc-tin-oxide buffer layer for enhancing heterojunction interface quality in metal-oxide solar cells. Energy and Environmental Science, 2013, 6, 2112.	30.8	160
27	Autonomous experimentation systems for materials development: A community perspective. Matter, 2021, 4, 2702-2726.	10.0	143
28	Improved Cu <sub>2</sub> Oâ€Based Solar Cells Using Atomic Layer Deposition to Control the Cu Oxidation State at the pâ€n Junction. Advanced Energy Materials, 2014, 4, 1301916.	19.5	142
29	Strongly Enhanced Photovoltaic Performance and Defect Physics of Air‣table Bismuth Oxyiodide (BiOI). Advanced Materials, 2017, 29, 1702176.	21.0	139
30	<i>A</i> -Site Cation in Inorganic <i>A</i> <sub>3</sub> Sb <sub>2</sub> I <sub>9</sub> Perovskite Influences Structural Dimensionality, Exciton Binding Energy, and Solar Cell Performance. Chemistry of Materials, 2018, 30, 3734-3742.	6.7	134
31	The capital intensity of photovoltaics manufacturing: barrier to scale and opportunity for innovation. Energy and Environmental Science, 2015, 8, 3395-3408.	30.8	133
32	Coâ€optimization of SnS absorber and Zn(O,S) buffer materials for improved solar cells. Progress in Photovoltaics: Research and Applications, 2015, 23, 901-908.	8.1	132
33	Engineering Solutions and Root-Cause Analysis for Light-Induced Degradation in <italic>p</italic> -Type Multicrystalline Silicon PERC Modules. IEEE Journal of Photovoltaics, 2016, 6, 860-868.	2.5	129
34	Hall mobility of cuprous oxide thin films deposited by reactive direct-current magnetron sputtering. Applied Physics Letters, 2011, 98, .	3.3	120
35	Triplet-Sensitization by Lead Halide Perovskite Thin Films for Near-Infrared-to-Visible Upconversion. ACS Energy Letters, 2019, 4, 888-895.	17.4	117
36	Phase transition-induced band edge engineering of BiVO <sub>4</sub> to split pure water under visible light. Proceedings of the National Academy of Sciences of the United States of America, 2015, 112, 13774-13778.	7.1	116

#	Article	IF	CITATIONS
37	Perovskite-Inspired Photovoltaic Materials: Toward Best Practices in Materials Characterization and Calculations. Chemistry of Materials, 2017, 29, 1964-1988.	6.7	116
38	Assessing the drivers of regional trends in solar photovoltaic manufacturing. Energy and Environmental Science, 2013, 6, 2811.	30.8	115
39	Nitrogen-doped cuprous oxide as a p-type hole-transporting layer in thin-film solar cells. Journal of Materials Chemistry A, 2013, 1, 15416.	10.3	108
40	Synchrotron-based investigations of the nature and impact of iron contamination in multicrystalline silicon solar cells. Journal of Applied Physics, 2005, 97, 074901.	2.5	100
41	Extended infrared photoresponse and gain in chalcogen-supersaturated silicon photodiodes. Applied Physics Letters, 2011, 99, .	3.3	100
42	Band offsets of <i>n</i> -type electron-selective contacts on cuprous oxide (Cu2O) for photovoltaics. Applied Physics Letters, 2014, 105, .	3.3	96
43	High Tolerance to Iron Contamination in Lead Halide Perovskite Solar Cells. ACS Nano, 2017, 11, 7101-7109.	14.6	90
44	Antimony-Doped Tin(II) Sulfide Thin Films. Chemistry of Materials, 2012, 24, 4556-4562.	6.7	88
45	Iron point defect reduction in multicrystalline silicon solar cells. Applied Physics Letters, 2008, 92, .	3.3	87
46	Solvent-Engineering Method to Deposit Compact Bismuth-Based Thin Films: Mechanism and Application to Photovoltaics. Chemistry of Materials, 2018, 30, 336-343.	6.7	87
47	AI Applications through the Whole Life Cycle of Material Discovery. Matter, 2020, 3, 393-432.	10.0	86
48	Two-step machine learning enables optimized nanoparticle synthesis. Npj Computational Materials, 2021, 7, .	8.7	86
49	Revisiting thin silicon for photovoltaics: a technoeconomic perspective. Energy and Environmental Science, 2020, 13, 12-23.	30.8	85
50	Technoeconomic model of second-life batteries for utility-scale solar considering calendar and cycle aging. Applied Energy, 2020, 269, 115127.	10.1	84
51	Selfâ€Powered Sensors Enabled by Wideâ€Bandgap Perovskite Indoor Photovoltaic Cells. Advanced Functional Materials, 2019, 29, 1904072.	14.9	83
52	Modeling the Cost and Minimum Sustainable Price of Crystalline Silicon Photovoltaic Manufacturing in the United States. IEEE Journal of Photovoltaics, 2013, 3, 662-668.	2.5	80
53	Discovery of temperature-induced stability reversal in perovskites using high-throughput robotic learning. Nature Communications, 2021, 12, 2191.	12.8	77
54	How machine learning can help select capping layers to suppress perovskite degradation. Nature Communications, 2020, 11, 4172.	12.8	75

#	Article	IF	CITATIONS
55	A data fusion approach to optimize compositional stability of halide perovskites. Matter, 2021, 4, 1305-1322.	10.0	75
56	Dislocation density reduction in multicrystalline silicon solar cell material by high temperature annealing. Applied Physics Letters, 2008, 93, .	3.3	74
57	Non-cubic solar cell materials. Nature Photonics, 2015, 9, 355-357.	31.4	73
58	The realistic energy yield potential of GaAs-on-Si tandem solar cells: a theoretical case study. Optics Express, 2015, 23, A382.	3.4	72
59	Lifetime Spectroscopy Investigation of Light-Induced Degradation in p-type Multicrystalline Silicon PERC. IEEE Journal of Photovoltaics, 2016, 6, 1466-1472.	2.5	70
60	Machine learning with knowledge constraints for process optimization of open-air perovskite solar cell manufacturing. Joule, 2022, 6, 834-849.	24.0	69
61	Economically sustainable scaling of photovoltaics to meet climate targets. Energy and Environmental Science, 2016, 9, 2122-2129.	30.8	68
62	Economic viability of thin-film tandem solar modules in the United States. Nature Energy, 2018, 3, 387-394.	39.5	68
63	Precursor Concentration Affects Grain Size, Crystal Orientation, and Local Performance in Mixed-Ion Lead Perovskite Solar Cells. ACS Applied Energy Materials, 2018, 1, 6801-6808.	5.1	65
64	Evolution of LeTID Defects in p-Type Multicrystalline Silicon During Degradation and Regeneration. IEEE Journal of Photovoltaics, 2017, 7, 980-987.	2.5	62
65	Benchmarking the performance of Bayesian optimization across multiple experimental materials science domains. Npj Computational Materials, 2021, 7, .	8.7	62
66	Enhancing the Infrared Photoresponse of Silicon by Controlling the Fermi Level Location within an Impurity Band. Advanced Functional Materials, 2014, 24, 2852-2858.	14.9	60
67	Interpretable and Explainable Machine Learning for Materials Science and Chemistry. Accounts of Materials Research, 2022, 3, 597-607.	11.7	60
68	Supersaturating silicon with transition metals by ion implantation and pulsed laser melting. Journal of Applied Physics, 2013, 114, .	2.5	59
69	Economically Sustainable Growth of Perovskite Photovoltaics Manufacturing. Joule, 2020, 4, 822-839.	24.0	59
70	An invertible crystallographic representation for general inverse design of inorganic crystals with targeted properties. Matter, 2022, 5, 314-335.	10.0	59
71	Interfaces between water splitting catalysts and buried silicon junctions. Energy and Environmental Science, 2013, 6, 532-538.	30.8	58
72	Roadmap for cost-effective, commercially-viable perovskite silicon tandems for the current and future PV market. Sustainable Energy and Fuels, 2020, 4, 852-862.	4.9	58

#	Article	IF	CITATIONS
73	How far does the defect tolerance of lead-halide perovskites range? The example of Bi impurities introducing efficient recombination centers. Journal of Materials Chemistry A, 2019, 7, 23838-23853.	10.3	57
74	Machine learning enables polymer cloud-point engineering via inverse design. Npj Computational Materials, 2019, 5, .	8.7	56
75	Variations of ionization potential and electron affinity as a function of surface orientation: The case of orthorhombic SnS. Applied Physics Letters, 2014, 104, .	3.3	52
76	Reactivation of sub-bandgap absorption in chalcogen-hyperdoped silicon. Applied Physics Letters, 2011, 98, .	3.3	49
77	The Value of Efficiency in Photovoltaics. Joule, 2019, 3, 2732-2747.	24.0	49
78	Rapid Photovoltaic Device Characterization through Bayesian Parameter Estimation. Joule, 2017, 1, 843-856.	24.0	47
79	Perovskite PV-Powered RFID: Enabling Low-Cost Self-Powered IoT Sensors. IEEE Sensors Journal, 2020, 20, 471-478.	4.7	46
80	Optimizing phosphorus diffusion for photovoltaic applications: Peak doping, inactive phosphorus, gettering, and contact formation. Journal of Applied Physics, 2016, 119, .	2.5	45
81	Targeted Search for Effective Intermediate Band Solar Cell Materials. IEEE Journal of Photovoltaics, 2015, 5, 212-218.	2.5	44
82	Energy-yield prediction for II–VI-based thin-film tandem solar cells. Energy and Environmental Science, 2016, 9, 2644-2653.	30.8	43
83	Deactivation of metastable single-crystal silicon hyperdoped with sulfur. Journal of Applied Physics, 2013, 114, .	2.5	41
84	Long Range Battery-Less PV-Powered RFID Tag Sensors. IEEE Internet of Things Journal, 2019, 6, 6989-6996.	8.7	41
85	Global Prediction of Photovoltaic Field Performance Differences Using Open-Source Satellite Data. Joule, 2018, 2, 307-322.	24.0	40
86	Dislocation formation in seeds for quasi-monocrystalline silicon for solar cells. Acta Materialia, 2014, 67, 199-206.	7.9	39
87	Energy Yield Limits for Single-Junction Solar Cells. Joule, 2018, 2, 1160-1170.	24.0	38
88	Stateâ€ofâ€ŧheâ€Art Electronâ€Selective Contacts in Perovskite Solar Cells. Advanced Materials Interfaces, 2018, 5, 1800408.	3.7	38
89	The effect of structural dimensionality on carrier mobility in lead-halide perovskites. Journal of Materials Chemistry A, 2019, 7, 23949-23957.	10.3	38
90	Organic Vapor Passivation of Silicon at Room Temperature. Advanced Materials, 2013, 25, 2078-2083.	21.0	37

#	Article	IF	CITATIONS
91	High-Performance and Traditional Multicrystalline Silicon: Comparing Gettering Responses and Lifetime-Limiting Defects. IEEE Journal of Photovoltaics, 2016, 6, 632-640.	2.5	36
92	Structural and Chemical Features Giving Rise to Defect Tolerance of Binary Semiconductors. Chemistry of Materials, 2018, 30, 5583-5592.	6.7	36
93	Meeting global cooling demand with photovoltaics during the 21st century. Energy and Environmental Science, 2019, 12, 2706-2716.	30.8	33
94	Optimization and design of a low-cost, village-scale, photovoltaic-powered, electrodialysis reversal desalination system for rural India. Desalination, 2019, 452, 265-278.	8.2	33
95	Analyses of the Evolution of Iron-Silicide Precipitates in Multicrystalline Silicon During Solar Cell Processing. IEEE Journal of Photovoltaics, 2013, 3, 131-137.	2.5	32
96	Numerical Analysis of Radiative Recombination and Reabsorption in GaAs/Si Tandem. IEEE Journal of Photovoltaics, 2015, 5, 1079-1086.	2.5	32
97	Stress effects on the Raman spectrum of an amorphous material: Theory and experiment on <mml:math xmlns:mml="http://www.w3.org/1998/Math/MathML"&gt;<mml:mi>a</mml:mi>-Si:H. Physical Review B, 2015, 92, .</mml:math 	3.2	30
98	Minority-carrier lifetime and defect content of n-type silicon grown by the noncontact crucible method. Journal of Crystal Growth, 2014, 407, 31-36.	1.5	29
99	Framework to predict optimal buffer layer pairing for thin film solar cell absorbers: A case study for tin sulfide/zinc oxysulfide. Journal of Applied Physics, 2015, 118, .	2.5	29
100	Adaptive power consumption improves the reliability of solar-powered devices for internet of things. Applied Energy, 2018, 224, 322-329.	10.1	28
101	Developing a Robust Recombination Contact to Realize Monolithic Perovskite Tandems With Industrially Common p-Type Silicon Solar Cells. IEEE Journal of Photovoltaics, 2018, 8, 1023-1028.	2.5	27
102	Advantages of operation flexibility and load sizing for PV-powered system design. Solar Energy, 2018, 162, 132-139.	6.1	27
103	Halide Heterogeneity Affects Local Charge Carrier Dynamics in Mixed-Ion Lead Perovskite Thin Films. Chemistry of Materials, 2019, 31, 3712-3721.	6.7	27
104	Extended X-ray absorption fine structure spectroscopy of selenium-hyperdoped silicon. Journal of Applied Physics, 2013, 114, 133507.	2.5	25
105	Building intuition of iron evolution during solar cell processing through analysis of different process models. Applied Physics A: Materials Science and Processing, 2015, 120, 1357-1373.	2.3	25
106	Transfer Learning-Based Artificial Intelligence-Integrated Physical Modeling to Enable Failure Analysis for 3 Nanometer and Smaller Silicon-Based CMOS Transistors. ACS Applied Nano Materials, 2021, 4, 6903-6915.	5.0	25
107	Synchrotron-based analysis of chromium distributions in multicrystalline silicon for solar cells. Applied Physics Letters, 2015, 106, .	3.3	24
108	On the methodology of energy yield assessment for one-Sun tandem solar cells. Solar Energy, 2016, 135, 598-604.	6.1	24

#	Article	IF	CITATIONS
109	Material requirements for the adoption of unconventional silicon crystal and wafer growth techniques for highâ€efficiency solar cells. Progress in Photovoltaics: Research and Applications, 2016, 24, 122-132.	8.1	24
110	Determining interface properties limiting open-circuit voltage in heterojunction solar cells. Journal of Applied Physics, 2017, 121, .	2.5	24
111	Thin silicon solar cells: Pathway to cost-effective and defect-tolerant cell design. Energy Procedia, 2017, 124, 706-711.	1.8	24
112	Field demonstration of a cost-optimized solar powered electrodialysis reversal desalination system in rural India. Desalination, 2020, 476, 114217.	8.2	24
113	Singleâ€Phase Filamentary Cellular Breakdown Via Laserâ€Induced Solute Segregation. Advanced Functional Materials, 2015, 25, 4642-4649.	14.9	23
114	Solubility and Diffusivity: Important Metrics in the Search for the Root Cause of Light- and Elevated Temperature-Induced Degradation. IEEE Journal of Photovoltaics, 2018, 8, 448-455.	2.5	23
115	Phosphonic Acid Modification of the Electron Selective Contact: Interfacial Effects in Perovskite Solar Cells. ACS Applied Energy Materials, 2019, 2, 2402-2408.	5.1	23
116	Synchrotron-based investigation of transition-metal getterability in <i>n</i> -type multicrystalline silicon. Applied Physics Letters, 2016, 108, .	3.3	22
117	A Two-Step Absorber Deposition Approach To Overcome Shunt Losses in Thin-Film Solar Cells: Using Tin Sulfide as a Proof-of-Concept Material System. ACS Applied Materials & Interfaces, 2016, 8, 22664-22670.	8.0	22
118	Improving the Carrier Lifetime of Tin Sulfide via Prediction and Mitigation of Harmful Point Defects. Journal of Physical Chemistry Letters, 2017, 8, 3661-3667.	4.6	22
119	A Worldwide Theoretical Comparison of Outdoor Potential for Various Silicon-Based Tandem Module Architecture. Cell Reports Physical Science, 2020, 1, 100037.	5.6	22
120	Identification of lifetime limiting defects by temperature- and injection-dependent photoluminescence imaging. Journal of Applied Physics, 2016, 120, .	2.5	20
121	Multiâ€Fidelity Highâ€Throughput Optimization of Electrical Conductivity in P3HTâ€CNT Composites. Advanced Functional Materials, 2021, 31, 2102606.	14.9	20
122	A Machine Learning and Computer Vision Approach to Rapidly Optimize Multiscale Droplet Generation. ACS Applied Materials & Interfaces, 2022, 14, 4668-4679.	8.0	20
123	Retrograde Melting and Internal Liquid Gettering in Silicon. Advanced Materials, 2010, 22, 3948-3953.	21.0	19
124	Origins of Structural Hole Traps in Hydrogenated Amorphous Silicon. Physical Review Letters, 2013, 110, 146805.	7.8	19
125	Sorting Metrics for Customized Phosphorus Diffusion Gettering. IEEE Journal of Photovoltaics, 2014, 4, 1421-1428.	2.5	19
126	X-ray absorption spectroscopy elucidates the impact of structural disorder on electron mobility in amorphous zinc-tin-oxide thin films. Applied Physics Letters, 2014, 104, .	3.3	19

#	Article	IF	CITATIONS
127	Making Record-efficiency SnS Solar Cells by Thermal Evaporation and Atomic Layer Deposition. Journal of Visualized Experiments, 2015, , e52705.	0.3	19
128	Controlling dopant profiles in hyperdoped silicon by modifying dopant evaporation rates during pulsed laser melting. Applied Physics Letters, 2012, 100, .	3.3	18
129	Predicting the outdoor performance of flat-plate Ill–V/Si tandem solar cells. Solar Energy, 2017, 149, 77-84.	6.1	18
130	The influence of nitrogen doping on the electrical and vibrational properties of Cu <sub>2</sub> O. Physica Status Solidi (B): Basic Research, 2017, 254, 1600421.	1.5	18
131	Embedding physics domain knowledge into a Bayesian network enables layer-by-layer process innovation for photovoltaics. Npj Computational Materials, 2020, 6, .	8.7	18
132	High-performance p-type multicrystalline silicon (mc-Si): Its characterization and projected performance in PERC solar cells. Solar Energy, 2018, 175, 68-74.	6.1	17
133	Sustainable silicon photovoltaics manufacturing in a global market: A techno-economic, tariff and transportation framework. Applied Energy, 2018, 212, 704-719.	10.1	17
134	The Impact of COVID-19-Related Measures on the Solar Resource in Areas with High Levels of Air Pollution. Joule, 2020, 4, 1681-1687.	24.0	17
135	Predicting Antimicrobial Activity of Conjugated Oligoelectrolyte Molecules via Machine Learning. Journal of the American Chemical Society, 2021, 143, 18917-18931.	13.7	17
136	Microscopic Distributions of Defect Luminescence From Subgrain Boundaries in Multicrystalline Silicon Wafers. IEEE Journal of Photovoltaics, 2017, 7, 772-780.	2.5	16
137	Persistent and adaptive power system for solar powered sensors of Internet of Things (IoT). Energy Procedia, 2017, 143, 739-741.	1.8	16
138	Spontaneous lateral phase separation of AlInP during thin film growth and its effect on luminescence. Journal of Applied Physics, 2015, 118, .	2.5	15
139	Nanohole Structuring for Improved Performance of Hydrogenated Amorphous Silicon Photovoltaics. ACS Applied Materials & Interfaces, 2016, 8, 15169-15176.	8.0	15
140	Highly tensile-strained Ge/InAlAs nanocomposites. Nature Communications, 2017, 8, 14204.	12.8	15
141	Detection of sub-500-μm cracks in multicrystalline silicon wafer using edge-illuminated dark-field imaging to enable thin solar cell manufacturing. Solar Energy Materials and Solar Cells, 2019, 196, 70-77.	6.2	15
142	Rapid dislocationâ€density mapping of asâ€cut crystalline silicon wafers. Physica Status Solidi - Rapid Research Letters, 2013, 7, 1041-1044.	2.4	14
143	Metal Grid Contact Design for Four-Terminal Tandem Solar Cells. IEEE Journal of Photovoltaics, 2017, 7, 934-940.	2.5	14
144	Design of a Submillimeter Crack-Detection Tool for Si Photovoltaic Wafers Using Vicinal Illumination and Dark-Field Scattering. IEEE Journal of Photovoltaics, 2018, 8, 1449-1456.	2.5	13

#	Article	IF	CITATIONS
145	Darwin at High Temperature: Advancing Solar Cell Material Design Using Defect Kinetics Simulations and Evolutionary Optimization. Advanced Energy Materials, 2014, 4, 1400459.	19.5	12
146	A Framework for Process-to-Module Modeling of a-Si/c-Si (HIT) Heterojunction Solar Cells to Investigate the Cell-to-Module Efficiency Gap. IEEE Journal of Photovoltaics, 2016, 6, 875-887.	2.5	12
147	Analysis of loss mechanisms in Ag2ZnSnSe4 Schottky barrier photovoltaics. Journal of Applied Physics, 2017, 121, .	2.5	12
148	<i>Tabula Rasa</i> for <i>n</i> z siliconâ€based photovoltaics. Progress in Photovoltaics: Research and Applications, 2019, 27, 136-143.	8.1	12
149	Enhanced charge carrier lifetime and mobility as a result of Rb and Cs incorporation in hybrid perovskite. Applied Physics Letters, 2021, 118, .	3.3	12
150	Using automated serendipity to discover how trace water promotes and inhibits lead halide perovskite crystal formation. Applied Physics Letters, 2021, 119, .	3.3	12
151	Investigation of Lifetime-Limiting Defects After High-Temperature Phosphorus Diffusion in High-Iron-Content Multicrystalline Silicon. IEEE Journal of Photovoltaics, 2014, 4, 866-873.	2.5	11
152	Solar Cell Efficiency and High Temperature Processing of n-type Silicon Grown by the Noncontact Crucible Method. Energy Procedia, 2016, 92, 815-821.	1.8	11
153	Solar research not finished. Nature Photonics, 2016, 10, 141-142.	31.4	11
154	Tuning Electrical, Optical, and Thermal Properties through Cation Disorder in Cu <sub>2</sub> ZnSnS <sub>4</sub> . Chemistry of Materials, 2019, 31, 8402-8412.	6.7	11
155	Increased Throughput and Sensitivity of Synchrotron-Based Characterization for Photovoltaic Materials. IEEE Journal of Photovoltaics, 2017, 7, 763-771.	2.5	10
156	Crack detection in crystalline silicon solar cells using dark-field imaging. Energy Procedia, 2017, 124, 526-531.	1.8	10
157	Ohmic shunts in two-terminal dual-junction solar cells with current mismatch. Japanese Journal of Applied Physics, 2017, 56, 08MA05.	1.5	10
158	Design of domestic photovoltaics manufacturing systems under global constraints and uncertainty. Renewable Energy, 2020, 148, 1174-1189.	8.9	10
159	Applications of novel effects derived from Si ingot growth inside Si melt without contact with crucible wall using noncontact crucible method to high-efficiency solar cells. Journal of Crystal Growth, 2017, 468, 705-709.	1.5	9
160	Voltage- and flow-controlled electrodialysis batch operation: Flexible and optimized brackish water desalination. Desalination, 2021, 500, 114837.	8.2	9
161	Representative identification of spectra and environments (RISE) using kâ€means. Progress in Photovoltaics: Research and Applications, 2021, 29, 200-211.	8.1	9
162	Environmental Stability of Crystals: A Greedy Screening. Chemistry of Materials, 2022, 34, 2545-2552.	6.7	9

#	Article	IF	CITATIONS
163	Device Architecture and Lifetime Requirements for High Efficiency Multicrystalline Silicon Solar Cells. Energy Procedia, 2015, 77, 225-230.	1.8	8
164	Distribution and Charge State of Iron Impurities in Intentionally Contaminated Lead Halide Perovskites. IEEE Journal of Photovoltaics, 2018, 8, 156-161.	2.5	8
165	Bayesim: A tool for adaptive grid model fitting with Bayesian inference. Computer Physics Communications, 2019, 239, 161-165.	7.5	8
166	Opportunities for machine learning to accelerate halide-perovskite commercialization and scale-up. Matter, 2022, 5, 1353-1366.	10.0	8
167	Assessing the Device-performance Impacts of Structural Defects with TCAD Modeling. Energy Procedia, 2015, 77, 8-14.	1.8	7
168	Three-Dimensional TCAD Modeling of Grain Boundaries in High-Efficiency Silicon Solar Cells. IEEE Journal of Photovoltaics, 2016, 6, 817-822.	2.5	7
169	xmlns:mml="http://www.w3.org/1998/Math/MathML" display="inline"> <mml:mrow><mml:mi>Zn</mml:mi><mml:mi mathvariant="normal"&gt;O<mml:mo>â^¶</mml:mo><mml:mi>Al</mml:mi><mml:mo></mml:mo><mml:mi>Al</mml:mi><mml:mo><td>:msub&gt;<n< td=""><td>ıml:mrow&gt;&lt;ı</td></n<></td></mml:mo></mml:mi </mml:mrow>	:msub> <n< td=""><td>ıml:mrow&gt;&lt;ı</td></n<>	ıml:mrow><ı
	mathvariant="normal">O2 <td>&gt;<mml:m< td=""><td>o&gt;/</td></mml:m<></td>	> <mml:m< td=""><td>o&gt;/</td></mml:m<>	o>/
170	A robust low data solution: Dimension prediction of semiconductor nanorods. Computers and Chemical Engineering, 2021, 150, 107315.	3.8	7
171	Exceeding 3 ms Minority Carrier Lifetime in n–type Non-contact Crucible Silicon. Energy Procedia, 2016, 92, 779-784.	1.8	6
172	Discovering equations that govern experimental materials stability under environmental stress using scientific machine learning. Npj Computational Materials, 2022, 8, .	8.7	6
173	Synchrotronâ€based microprobe investigation of impurities in raw quartzâ€bearing and carbonâ€bearing feedstock materials for photovoltaic applications. Progress in Photovoltaics: Research and Applications, 2012, 20, 217-225.	8.1	5
174	Two-Step Annealing Study of Cuprous Oxide for Photovoltaic Applications. IEEE Journal of Photovoltaics, 2015, 5, 1476-1481.	2.5	5
175	Effect of layer thickness on device response of silicon heavily supersaturated with sulfur. AIP Advances, 2016, 6, .	1.3	5
176	Characterization of high-quality kerfless epitaxial silicon for solar cells: Defect sources and impact on minority-carrier lifetime. Journal of Crystal Growth, 2018, 483, 57-64.	1.5	5
177	How Much Physics is in a Current–Voltage Curve? Inferring Defect Properties From Photovoltaic Device Measurements. IEEE Journal of Photovoltaics, 2020, 10, 1532-1537.	2.5	5
178	An Open Combinatorial Diffraction Dataset Including Consensus Human and Machine Learning Labels with Quantified Uncertainty for Training New Machine Learning Models. Integrating Materials and Manufacturing Innovation, 2021, 10, 311-318.	2.6	5
179	Analysis of CdTe photovoltaic cells for ambient light energy harvesting. Journal Physics D: Applied Physics, 2020, 53, 405501.	2.8	5
180	Tailoring capping-layer composition for improved stability of mixed-halide perovskites. Journal of Materials Chemistry A, 2022, 10, 2957-2965.	10.3	5

#	Article	IF	CITATIONS
181	Do grain boundaries matter? Electrical and elemental identification at grain boundaries in LeTID-affected \$p\$-type multicrystalline silicon. , 2017, , .		4
182	Quantitative Specifications to Avoid Degradation during E-Beam and Induced Current Microscopy of Halide Perovskite Devices. Journal of Physical Chemistry C, 2020, 124, 18961-18967.	3.1	4
183	Seeding of Silicon Wire Growth by Outâ€Ðiffused Metal Precipitates. Small, 2011, 7, 563-567.	10.0	3
184	Electrically-inactive phosphorus re-distribution during low temperature annealing. Journal of Applied Physics, 2018, 123, 161535.	2.5	3
185	How changes in worldwide operating conditions affect solar cell performance. Solar Energy, 2021, 220, 671-679.	6.1	3
186	Combined Impact of Heterogeneous Lifetime and Gettering on Solar Cell Performance. Energy Procedia, 2015, 77, 119-128.	1.8	2
187	Sensitivity Analysis of Optical Metrics for Spectral Splitting Photovoltaic Systems: A Case Study. IEEE Journal of Photovoltaics, 2015, 5, 1380-1388.	2.5	2
188	Ultra-Thin GaAs Double-Junction Solar Cell With Carbon-Doped Emitter. IEEE Journal of Photovoltaics, 2018, 8, 1627-1634.	2.5	2
189	Moving Beyond p-Type mc-Si: Quantified Measurements of Iron Content and Lifetime of Iron-Rich Precipitates in n-Type Silicon. IEEE Journal of Photovoltaics, 2018, 8, 1525-1530.	2.5	2
190	Detecting Microcracks in Photovoltaics Silicon Wafers using Varitional Autoencoder. , 2020, , .		2
191	High-temperature diffusion processes in ultrafine-grained aluminum and its composites containing multi-walled carbon nanotubes. Journal of Composite Materials, 2015, 49, 2705-2711.	2.4	1
192	Evaluating root cause: the distinct roles of hydrogen and firing in activating light- and elevated-temperature induced degradation. , 2018, , .		1
193	Technoeconomic Analysis of Photovoltaics Module Manufacturing with Thin Silicon Wafers. , 2019, , .		1
194	Stress and temperature coupling effects on dislocation density reduction in multicrystalline silicon. , 2010, , .		0
195	Thin Films: Organic Vapor Passivation of Silicon at Room Temperature (Adv. Mater. 14/2013). Advanced Materials, 2013, 25, 2077-2077.	21.0	0
196	In situ PL imaging toward real-time plating process control. , 2014, , .		0
197	Process-to-panel modeling of a-Si/c-Si heterojunction solar cells. , 2015, , .		0
198	Vertically integrated modeling of light-induced defects: Process modeling, degradation kinetics and device impact. AIP Conference Proceedings, 2018, , .	0.4	0